Examining the Potential of Sandy Marine Sediments Surrounding Giant Kelp Forests to Provide Recycled Nutrients for Growth

Heili E. Lowman[†]*, Mare E. Hirsch[‡], Mark A. Brzezinski[†§], and John M. Melack[†]

[†]Department of Ecology, Evolution, and Marine Biology
University of California, Santa Barbara
Santa Barbara, CA 93106, U.S.A.

[‡]Media Arts and Technology Graduate Program
University of California, Santa Barbara
Santa Barbara, CA 93106, U.S.A.

[§]Marine Science Institute
University of California, Santa Barbara
Santa Barbara, CA 93106, U.S.A.

www.cerf-jcr.org

www.JCRonline.org

ABSTRACT

Lowman, H.E.; Hirsch, M.E.; Brzezinski, M.A., and Melack, J.M., 2023. Examining the potential of sandy marine sediments surrounding giant kelp forests to provide recycled nutrients for growth. *Journal of Coastal Research,* 39(3), 442–454. Charlotte (North Carolina), ISSN 0749-0208.

Permeable marine sediments are biogeochemically active and may contribute dissolved nutrients to support primary production in coastal regions. This study examined the potential of permeable marine sediments near giant kelp forests in the Santa Barbara Channel, California as a source of ammonium (NH_4^+) to the overlying water column to support the observed growth of kelp during summer months when nitrate availability is low. Several nearshore sites located in coastal California in $<$20 m water depth were sampled for porewater nutrient concentrations, flushing rates, and nutrient fluxes in addition to diel fluctuations in nutrient concentrations of the overlying water column. Time-series analyses of porewater temperatures indicate that porewater flushed to a depth of 15 cm approximately every two hours, and mean NH_4^+ concentrations of porewater at these depths was 40 μM. The results of flow-through bioreactor incubations indicate that the top 2 cm of sediment are a net source of dissolved nitrogen to the overlying water column and are capable of supplying from 0.05 to 0.90 mmol $NH_4^+\,m^{-2}\,day^{-1}$. Diel water sampling demonstrates that kelp forests may be exposed to NH_4^+ concentrations greater than 1 μM for multiple hours (four–eight) over a day. These measured reservoirs and exchange rates of NH_4^+ suggest sandy marine sediments provide a significant source of nitrogen to the water column and may help meet the nitrogen demand by giant kelp during summer in the Santa Barbara Channel.

ADDITIONAL INDEX WORDS: *Nitrogen, ammonium, remineralization, porewater, Santa Barbara Channel.*

INTRODUCTION

Permeable, sandy marine sediments can be overlooked as sites of biogeochemical activity due to their low organic matter content (Boudreau *et al.*, 2001), but recent work suggests these sediments may supply nutrients to overlying water due to regeneration of dissolved nutrients and rapid porewater exchange (Cai *et al.*, 2020; Rocha, 2008). These findings are particularly pertinent to coastal marine regions as nearshore sediments along the continental shelf are typically coarser than offshore sediment (Huettel, Berg, and Kotska, 2014). As permeability increases in coarser sediment, it can have a significant effect on biogeochemical rates (Huettel, Berg, and Kotska, 2014; Marchant *et al.*, 2016) due to the advective flow of porewater (Janssen, Huettel, and Witte, 2005). This advective flow creates heterogeneous regions of oxygenation and organic material accumulation and, due to resulting oscillations of the redox boundary, may enable coupling of oxic-anoxic processes (Marchant *et al.*, 2016; Rocha, 2008). Permeable sediments contain microbial cell numbers that are approximately 1000 times greater than in a similar volume of overlying seawater

(Huettel, Berg, and Kotska, 2014), and sediment biogeochemistry is further influenced by burrowing and bioturbating meiofaunal communities, which can further structure microbial communities (Rocha, 2008). In summary, permeability, porewater circulation, and *in situ* biological communities enable nearshore permeable marine sediments to remineralize significant quantities of organic material and contribute nutrients and inorganic carbon to coastal marine waters (Huettel, Berg, and Kotska, 2014).

Sediment horizons that exchange porewater with the overlying water column are particularly well-positioned to remineralize organic material and detritus at high rates (de Beer *et al.*, 2005). Physical exchange of porewater with overlying waters occurs due to pressure gradients created by currents, tides, or waves (Janssen, Huettel, and Witte, 2005). This exchange leads to the increased delivery of both oxygen and organic material into sediments (Janssen, Huettel, and Witte, 2005; Rocha, 2008). As a result, sediment redox structure is a function of both porewater exchange and organic matter loading (Cai *et al.*, 2020; Falter and Sansone, 2000). Greater organic matter loading promotes oxygen consumption, while advective flows simultaneously recharge oxygen and organic matter, particularly in the top 20 cm of sediment (Huettel, Berg, and Kotska, 2014).
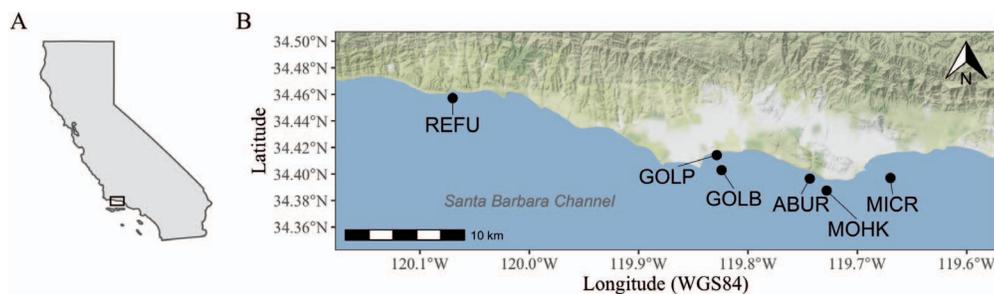
Figure 1. State of California, U.S.A. with inset location bounded by a black rectangle (panel A). Region of the Santa Barbara Channel, California, U.S.A. where sampling sites were located (panel B). Kelp forest reef and pier locations denoted by black dots.

Due to the supply of organic matter and oxygen coupled with rapid microbial remineralization rates, permeable marine sediments can be a significant source of inorganic nitrogen to the overlying water (Kitidis et al., 2017; Rowe, Clifford, and Smith, 1975). In certain systems, marine sediments have been demonstrated to supply over 30% of pelagic nitrogen demand (Boynton et al., 2018), including ammonium (NH_4^+), which is the preferred form of nitrogen for phytoplankton (Glibert et al., 2016). Few studies provide evidence of NH_4^+ uptake by sediments (Boynton et al., 2018), suggesting marine sediments are more often a source than a sink of NH_4^+. In addition, advective flow of porewater has been demonstrated to increase the release of NH_4^+ from sediments before it can be taken up by nitrifiers (Cook et al., 2006; Kessler et al., 2012). Once released into the water column, NH_4^+ cycles rapidly in marine environments (Capone et al., 2008). Further investigation of NH_4^+ cycling in marine waters and permeable sediments is warranted since NH_4^+ is in high demand by phototrophs, for use in primary production, and by nitrifiers, as the substrate for nitrification (Gustafsson and Norkko, 2016).

The sites examined in this study are situated in nearshore marine environments of the Santa Barbara Channel (SBC), where nitrate (NO_3^-) concentrations in the water column are greater in winter and spring due to runoff from storms and upwelling but remain below the limit of detection (0.2 μM) for much of the summer and into the fall (July–November) (Brzezinski et al., 2013; McPhee-Shaw et al., 2007). Despite the apparent low NO_3^- availability during summer, nearshore forests of Macrocystis pyrifera (giant kelp) continue to have high rates of net primary production (Brzezinski et al., 2013; Reed et al., 2016). Giant kelp cannot store nitrogen reserves for longer than a few weeks (Gerard, 1982a; Wheeler and North, 1980), so a persistent source of nitrogen is critical for its growth. Models of giant kelp growth, and the nitrogen uptake needed to sustain it, suggest that during summer months in the SBC, 50% of nitrogen used by kelp is provided by a form other than NO_3^- (Fram et al., 2008).

In the SBC, giant kelp can take up additional forms of dissolved nitrogen, specifically NH_4^+ and urea, and uptake rates in giant kelp decline less at night than uptake rates by phytoplankton, potentially conferring a competitive advantage during low-nutrient conditions (Smith et al., 2020; Smith et al., 2018). The ability of giant kelp to uptake dissolved organic forms of nitrogen (i.e. urea) also suggest the possibility of remineralization of organic matter providing additional routes of nutrient supply to support kelp growth. Cedeno et al. (2021) have demonstrated giant kelp's ability to rapidly take up NH_4^+ during pulse events, suggesting brief periods of exposure to higher NH_4^+ concentrations could help to offset otherwise low-nutrient conditions. The primary hypotheses examined in this project are whether permeable marine sediments around giant kelp forests serve as a net source of NH_4^+ and whether rates of NH_4^+ efflux from sediments are high enough to contribute significantly to measured seawater nutrient concentrations, supplementing low NO_3^- during summer months. This study combines in situ seawater and porewater measurements with a series of flow-through sediment bioreactors to investigate the rate at which these marine sediments might supply NH_4^+ to the overlying water column during the stratified summer season, when kelp growth rates are highest and NO_3^- concentrations are lowest.

METHODS

In summer 2016, sediment porewater and seawater nutrient concentrations in giant kelp forests were measured, and instrumentation was deployed in kelp forest sediment to measure porewater temperatures. In the subsequent three summers (2017–2019), sediment cores were incubated using a flow-through bioreactor protocol to measure dissolved nutrient effluxes from kelp forest sediment. Additional sediment cores were collected during different seasons spanning the study (2015–2017) for sediment characteristics, and a nearshore seawater sampling campaign was conducted in summer 2018 to measure diel fluctuations in dissolved nutrients.

Site Description

Five kelp forest sites located in the Santa Barbara Channel were studied: Refugio (REFU, 34° 27.432 N, 120° 4.2 W), Goleta Bay (GOLB, 34° 24.175 N, 119° 49.450 W), Arroyo Burro (ABUR, 34° 23.623 N, 119° 44.608 W), Mohawk (MOHK, 34° 23.251 N, 119° 43.685 W), and Mission Creek (MICR, 34° 23.821 N, 119° 40.185 W) (Figure 1). The Arroyo Burro and Mohawk sites are routinely sampled as part of the Santa Barbara Coastal Long Term Ecological Research (SBC LTER) program for dissolved and particulate constituents and the Goleta Bay, Arroyo Burro, and Mohawk sites are routinely sampled for giant kelp net primary production (Santa Barbara Coastal

LTER, Reed, and Miller, 2022; Santa Barbara Coastal LTER *et al.*, 2021b). Diel sampling took place on the Goleta pier (GOLP, 34° 24.85 N, 119° 49.715 W) due to ease of access over 24 hour periods (Figure 1). The pier has moderate boating and fishing traffic and extends approximately 500 m into Goleta Bay, bordered by Goleta Slough and Goleta beach park to the north and the SBC to the south. The sampling location was located approximately 300 m from shore, and water depth ranged from 5 to 8 m depending on the tide, similar to the depth zone occupied by giant kelp.

Oceanographic conditions in the SBC have three seasons: seasonal upwelling of cold, nutrient-rich water in spring (April–June), warm, stratified water in summer and fall (July–November), and episodic runoff from streams during winter storms (December–March) (Aguilera and Melack, 2018; Brzezinski *et al.*, 2013). Sampling was conducted during the warm, stratified summer period at all sites. Nearshore cross-shelf currents near the bottom average approximately 0.01 to 0.02 m s^{-1} with offshore flow (southward) (Fewings, Washburn, and Ohlmann, 2015). The summer wave base in the SBC, *i.e.* the water depth to which marine sediment may be disturbed or resuspended due to waves, is up to 20 m (Sommerfield, Lee, and Normark, 2009). Organic matter reaching the seafloor in these regions consists of a mix of marine and terrestrially derived organic material (Lowman *et al.*, 2021b; Page *et al.*, 2008). Sediment depth in this region of the SBC ranges from exposed bedrock (0 m) to 15 m (Sommerfield, Lee, and Normark, 2009).

Porewater Nutrient Concentrations and Temperature

Information regarding *in situ* conditions was first collected as sediment cores and water samples to aid in the later investigation of sediment nutrient fluxes using bioreactor incubations (Santa Barbara Coastal LTER *et al.*, 2018b,c). In June 2016, three replicate sediment cores (5 cm diameter × 20 cm long) were collected by SCUBA divers using hand corers fashioned from polycarbonate pipe and rubber stoppers at the Arroyo Burro, Mission Creek, and Refugio kelp forest sites at 15 m depth. In August 2016, additional sediment cores, three replicates per location, were collected at the Mohawk kelp forest site at 5, 7, 10, 15, and 20 m depths.

At each sampling location, water samples from the overlying water column were also collected by SCUBA divers using syringes; three samples were collected at each location: one at ~1 m water depth, one in the middle of the water column, and one ~50 cm above the sediment surface. Water samples were filtered through GF/F filters (0.7 μm, Whatman) into 20 mL high-density polyethylene (HDPE) vials aboard the boat and were transported in ice-filled coolers. According to Santa Barbara Coastal LTER protocol, HDPE sample vials were acid washed (10% HCl) prior to use and several rinses of seawater were performed prior to filtered sample collection (Santa Barbara Coastal LTER *et al.*, 2021b).

Upon return to shore, sediment cores were immediately sectioned into approximately 2 cm intervals. This process involved extruding the core using a plunger inserted into the core housing where the bottom stopper had previously been and pushing out the core, sectioning from top to bottom. Care was taken to place each section in a water-tight container so as to contain as much porewater as possible. Each core section was then homogenized, and 15 to 30 g of sediment from each section was placed in a 20 mL HDPE vial with perforations in the bottom and fitted into a larger plastic centrifuge tube, so that porewater could drip through the vial perforations into the centrifuge tube. All samples were centrifuged at 5000 rpm for 5 minutes, and the resulting porewater collected in the tubes was filtered through GF/C filters (1.2 μm, Whatman) and stored frozen (–20 °C).

During the summer of 2016, an array of temperature loggers (Tidbit, Onset Computer Corporation, Bourne, MA; precision, 0.2 °C) was deployed at the Mohawk kelp forest site. Four loggers were attached to a fiberglass pole using stainless steel screws and covered with anti-fouling tape. The array was buried in the sediment with loggers positioned at 5, 15, and 30 cm sediment depth as well as 50 cm above the seafloor. The full array was deployed on 8 August by a team of SCUBA divers and was recovered on 1 September 2016. Data collected by the array were analyzed starting on 10 August to allow time for the sediment and porewater horizons surrounding the array to reestablish and equilibrate.

Marine Sediment Core Sampling for Sediment Characteristics

Additional marine sediment cores were collected during four sampling campaigns in December 2015, June 2016, March 2017, and June 2017. Four replicate sediment cores (5 cm diameter × 20 cm long) were collected the Refugio, Goleta Bay, Arroyo Burro, Mohawk, and Mission Creek kelp forest sites by SCUBA divers at 20 m water depth using the hand corers described above. Additional information regarding sampling protocols is provided in Lowman *et al.* (2021b).

Bioreactor Design, Sediment Core Collection, and Incubations

To estimate dissolved nutrient effluxes from nearshore sediments, a closed-system, flow-through bioreactor was developed to mimic *in situ* conditions in sediments surrounding kelp forests. The bioreactor's use of sediment cores created fewer experimental artifacts than sediment slurries by keeping sediments, and their associated microbial and meiofaunal communities, intact (Pallud *et al.*, 2007). Only the top 2 cm of sediment was used to be certain these communities were habituated to oxic conditions, and a shorter sediment core decreased the chances of establishing either preferential flowpaths or microbial/redox gradients within the sediment in the chambers (Roychoudhury, Viollier, and Van Cappellen, 1998). Furthermore, the study design incorporated advective flow of porewater from the top to the bottom of the sediment core, because porewater temperatures tracked overlying water column temperatures closely (Figure 2) suggesting flow in this region is primarily driven by overlying wave and tidal pumping.

Sediment cores to be used in the bioreactor experiments were collected from the Goleta Bay, Arroyo Burro, and Mission Creek sites in August 2017, 2018, and 2019. At all three kelp forests, four replicate sediment cores (5 cm diameter × 20 cm long) were collected by SCUBA divers at 20 m water depth using hand corers; seawater was also collected into 2L HDPE bottles by divers from approximately 1 m above the sea floor. All samples were transported in ice-filled coolers to the
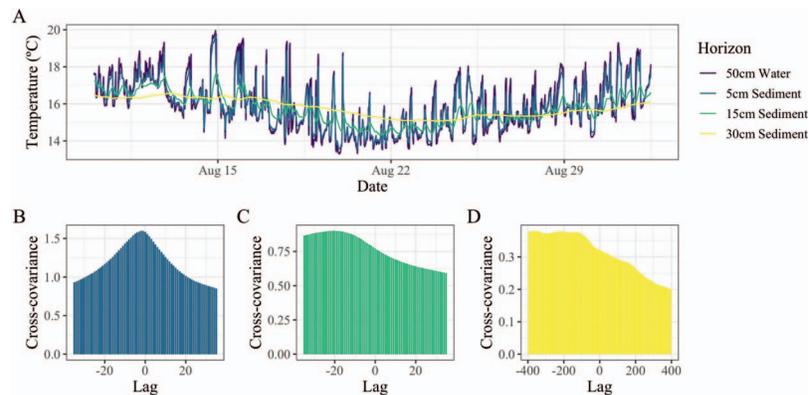
Figure 2. Sediment porewater temperature measured at Mohawk Reef (34° 23.251 N, 119° 43.685 W) using Tidbit temperature loggers in August 2016 (Santa Barbara Coastal LTER *et al.*, 2018c). Panel A displays the full dataset, while panels B through D display the cross-covariance between temperature at a given depth in the sediment versus the overlying water (B, C, and D refer to 5 cm, 15 cm, and 30 cm depths, respectively). Lags are denoted by the time step at which the data was collected (every 5 minutes). Therefore, a lag value of –10 refers to a 50 minute delay.

laboratory. Sediment cores were stored overnight (20 hour maximum) in a flow-through seawater tank with the top section exposed to maintain oxygenation and in situ temperatures in the porewater. Seawater samples remained unfiltered and were stored overnight in a 4 °C cold room.

Flow-through bioreactors were built using a modified design of the flow-through plug setup developed by Roychoudhury, Viollier, and Van Cappellen (1998). In 2017, a series of five bioreactors were used to conduct sediment efflux measurements with a section of PVC pipe used as a container for the sediment core, fit between two hand-cut acrylic end-pieces that were secured using zip ties. Each bioreactor housed one sediment core sample and was designed to connect to a seawater reservoir via a peristaltic pump that would pump water through the core in a recirculating, closed-loop fashion. Bioreactors were assembled with a combusted GF/B filter on the bottom end piece of each setup to prevent sediment from eroding into the reservoirs and clogging the tubing. One bioreactor housing was used as a control containing only seawater, and the remaining four were used to house sediment core replicates, henceforth referred to as the experimental replicates. In 2018, eight acrylic bioreactors were fabricated using an 80W laser cutter (Trotect Speedy 300 Laser Engraver), which allowed for greater precision and replication of the flow-through design. These bioreactors allowed for silicone bands to connect the PVC pipe containing the sediment core to each acrylic end-piece, creating an aligned seal (Appendix Figure 1). In 2018 and 2019, four replicates were run for both control (*i.e.* containing only seawater) and experimental bioreactors (*i.e.* containing both seawater and sediment).

Following overnight storage, sediment cores were removed from the seawater tank, and the top 2 cm of each replicate core was extruded, sectioned, and placed intact into a bioreactor, taking care not to compress or shear the surface of the core. The core depth was chosen to be 2 cm since that size was used in other flow-through bioreactor studies (*e.g.*, Ahmerkamp *et al.*,

2017; Laverman *et al.*, 2012; Pallud and Van Cappellen, 2006), and the design aimed to sample an oxic horizon. In addition, flow through the bioreactors was designed to progress from the top to the bottom of the core to use gravity to allow porewater to percolate through the sediment. The top to bottom flow design also mimics *in situ* conditions, where advective flow of porewater is primarily driven by overlying wave and tidal pumping rather than underlying groundwater infiltration (see Figure 2). Control bioreactors were assembled in the same fashion, including the filter on the bottom fitting, but without sediment.

All replicates were sealed and attached to a series of peristaltic pumps using PTFE tubing. Unfiltered seawater, which had been warmed to *in situ* temperature, was flushed through the bioreactors for 1 hour at approximately 5.5 mL min^{-1}. Each setup was allowed to drip freely during this period to allow existing porewater and dissolved nutrients to be flushed out. Flushing time was determined by a series of breakthrough curve analyses during which nutrient concentrations of water exiting the core were measured until they decreased to the same order of magnitude as the inflowing seawater. After flushing, each bioreactor was attached to a new reservoir of unfiltered seawater, which was held in a 15 °C water bath, and the entire setup was run in a recirculating fashion for three hours at the same rate as the initial flushing (5.5 mL min^{-1}). This flushing rate was used, because it exchanged existing porewater approximately every two minutes, a rate faster than the rate of exchange measured *in situ* at 5 cm depth (every 10 minutes, see Figure 2B). A series of tests using an oxygen sensor confirmed that oxygen concentrations in the reservoirs were not depleted during the three-hour period (*i.e.* dissolved oxygen did not decrease more than 1 mg L^{-1}). At the conclusion of each trial, an aliquot of the seawater in each reservoir was filtered through a GF/F filtered (0.7 µm, Whatman) for nutrient analyses. All cores used in the bioreactor setup were then frozen (–20 °C) for water content analyses to supplement sediment characteristics analyzed.

Diel Water Sampling

Water sampling was performed at the Goleta pier site over three 36-hour sampling periods in August 2018 with samples collected every four hours, beginning at 0600 the first morning and concluding at 1800 the following day. The three campaigns took place over the course of approximately one week to incorporate neap, midway, and spring tide conditions on August 3, 7, and 10, respectively. Information on tidal heights was from the gauge at site 9411340 (Longitude 119.685° W, Latitude 34.401° N) in Santa Barbara, California, U.S.A. maintained by National Oceanographic and Atmospheric Administration (NOAA, 2020). Prior to each water sampling, a vertical profile of the entire water column was obtained using a SBE 19plus V2 SeaCAT Profiler sampling at 4Hz (4 scans s^{-1}) to define the physical structure of the water column. Temperature readings using this instrument are accurate to 0.01 °C, and conductivity readings are accurate to 0.001 S m^{-1}. This instrument maintains pump-controlled, ducted flow to match the time constants of temperature and conductivity sensors and reduce salinity spiking. Water samples were collected using a 5 L Okeanus GO-FLO sampler at 1, 3, and 5 m depths, one deployment for each depth, taking care not to disturb the underlying sediments. Sample collection followed the Santa Barbara Coastal LTER protocol detailed above (Santa Barbara Coastal LTER *et al.*, 2021b). Immediately upon collection, samples were placed on ice in coolers, transported back to the laboratory, and filtered through GF/F filters (0.7 μm, Whatman) for nutrient analyses and MCE filters (0.45 μm, Millipore) for chlorophyll analyses.

Sample Analyses

Unfrozen seawater and porewater samples were analyzed for ammonium (NH_4^+) using the *ortho*-phthaldialdehyde method (Holmes *et al.*, 1999; Taylor *et al.*, 2007) and a Turner Trilogy Laboratory fluorometer (limit of detection, 0.05 μM). Standard curves were created using artificial seawater in 2016 and using low nutrient SBC seawater that had been incubated for over six months in 2017–2019. Frozen samples (–20 °C) were thawed and analyzed for combined nitrate (NO_3^-) and nitrite (NO_2^-) via flow injection analysis on a Lachat QuickChem 8500 Series 2 Analyzer (Hach Company, limit of detection, 0.50 μM in 2017 and 0.20 μM in 2018–2019). Another subset of samples was acidified using 4N HCl, refrigerated (4 °C), and analyzed for total dissolved nitrogen (TDN, limit of detection, 2 μM, precision, 1–2 μM) via high temperature combustion on a Shimadzu TOC-V Analyzer. TDN is interpreted as a combined value of dissolved inorganic nitrogen species (NH_4^+, NO_3^-, NO_2^-) and the numerous compounds considered dissolved organic nitrogen (DON). Samples were not assayed for TDN in 2017 due to an instrument malfunction and sample contamination. Frozen Mixed Cellulose Ester (MCE) filters were analyzed for chlorophyll by extraction in 90% acetone (Smith, Baker, and Dustan, 1981; Strickland and Parsons, 1968) and measurement on a Turner 10AU fluorometer (limit of detection, 0.02 μg L^{-1}). Chlorophyll *a* values were corrected for phaeopigments. For all analyses, if a measured concentration fell below the limit of detection, results are reported at the limit of detection.

For sediment cores used in the bioreactor incubations, two replicates were chosen from each site every year, and sediment water content was determined by drying approximately 2 g of thawed sediment at 60 °C for 48 hours. For sediment cores collected at additional sites between 2015 and 2017, sediment organic matter content was determined by drying 2 g of thawed sediment at 60 °C for 48 hours followed by combustion at 450 °C for four hours. Carbon and nitrogen content was determined by removing shells and coarse material from thawed sediment samples, drying at 60 °C for 48 hours, and grinding using a mortar and pestle. This material was then placed in silver capsules, acidified with 6% sulfurous acid, redried at 60 °C for 48 hours, and finally analyzed on a Thermos Finnigan Delta-Plus Advantage isotope mass spectrometer coupled with a Costech EAS elemental analyzer housed at the University of California Santa Barbara Marine Science Institute Analytical Laboratory. Grain size was determined by drying 20 g of thawed sediment at 60 °C for 48 hours, treating the samples with 5% sodium hexametaphosphate for 24 hours (Poppe *et al.*, 2000), and analyzing the samples on a Cilas laser diffraction particle size analyzer. Clay, silt, and sand fractions were determined using the cumulative values at 3.9 μm, between 3.9 μm and 62.5 μm, and greater than 62.5 μm, respectively. Additional information regarding analysis protocols is provided in Lowman *et al.* (2021b).

Data Analyses

Data organization and analyses of all data were performed using Excel (v 16.24) and R Statistical Software (v 4.0.4) (R Core Team, 2021). Data formatting and visualization were performed using the *tidyverse* package in RStudio (v 1.4.1106) (Wickham *et al.*, 2019). Maps were created using the *ggmap*, *ggspatial*, *sf*, and *USAboundaries* packages in R (Dunnington, 2020; Kahle and Wickham, 2013; Mullen and Bratt, 2018; Pebesma, 2018). The code used to run the analyses and generate all figures are available at https://github.com/ hlowman/sediment-nuts-2021. Values reported following a "±" symbol denote standard deviation, unless otherwise stated.

Following the sediment bioreactor incubations, net fluxes refer to the fluxes generated by the sediment alone. To determine net fluxes, the rate of change in nutrient concentrations (μM) measured in the reservoirs was calculated and divided by the length of the experiment (three hours). For each bioreactor experiment, the mean rates of change by control (seawater) and experimental (sediment core) treatments were calculated, using only the replicates of each treatment that successfully completed the full three-hour trial. For each site-year, the net change in concentration from sediment alone was determined by subtracting the mean rate of change of control incubations from the mean rate of change of experimental incubations. Net changes in nutrient concentrations were scaled to a larger surface area of benthos (1 m^2) and converted to net nutrient fluxes (μmol m^{-2} hr^{-1}) using the volume of the seawater reservoirs (250 mL) and the surface area of the sediment cores (19.6 cm^2).

Vertical water column profiles collected during diel sampling in August 2018 were processed and converted to .mat file formats using SBE data processing software (v 7.26.7).

Table 1. *Mean porewater ammonium concentrations (μM) plus or minus one standard deviation reported in sediment cores collected near kelp forest sites (Arroyo Burro = ABUR, Mission Creek = MICR, Refugio = REFU, Mohawk = MOHK) in June and August 2016 (Santa Barbara Coastal LTER et al., 2018b). Sediment depth reported in 2 cm horizons until 10 cm depth and then in a 5 cm horizon.*

Depth (cm)	ABUR 15 m	MICR 15 m	REFU 15 m	MOHK				
				5 m	7 m	10 m	15 m	20 m
0–2	45.2 ± 18.9	44.0 ± 22.1	61.8 ± 26.4	50.9 ± 11.7	12.9 ± 2.5	33.5 ± 5.1	54.7 ± 20.0	14.0 ± 7.5
2–4	59.1 ± 22.6	66.7 ± 3.2	42.6 ± 18.3	53.3 ± 27.8	20.8 ± 3.3	51.4 ± 19.5	51.3 ± 4.0	19.9 ± 4.2
4–6	65.8 ± 27.1	47.1 ± 9.7	46.0 ± 16.7	49.5 ± 11.4	18.3 ± 4.2	47.2 ± 16.6	53.8 ± 7.6	19.6 ± 8.6
6–8	66.2 ± 26.9	41.3 ± 15.3	53.0 ± 24.7	66.0 ± 6.0	23.0 ± 0.1	54.1 ± 31.1	53.5 ± 4.9	25.7 ± 4.6
8–10	—	36.5 ± 10.9	—	49.6 ± 21.0	25.2 ± 6.0	28.5 ± 25.3	56.5 ± 4.9	26.5 ± 13.7
10–15	—	—	—	53.4 ± 14.7	19.8 ± 4.5	31.4 ± 8.4	44.6 ± 10.8	34.6 ± 5.7

Arroyo Burro = ABUR, Mission Creek = MICR, Refugio = REFU, Mohawk = MOHK

Physical measurements were edited to remove spiking, and data were binned into 10 cm intervals.

Linear mixed effects models were created to determine the effect of experimental treatments on nutrient fluxes from sediment bioreactors and to determine the effect of environmental variables on NH_4^+ concentrations measured during diel sampling. For the first set of models, nutrient concentrations measured during bioreactor incubations were standardized by subtracting the mean concentration and dividing by the standard deviation of the concentration (*i.e.* z-scores). For the second model, NH_4^+ and chlorophyll *a* (chl *a*) concentrations measured during diel water sampling were log-transformed. Model creation began with fixed effects and random effects using a random intercept structure, which accounted for the repeated-measures design of both experiments. Model selection followed the protocol outlined by Zuur (2009, chapter 5), beginning with a linear model, accounting for variance structure, optimizing the fixed structure if appropriate, and validating the best model fit using distribution of residuals and Akaike Information Criterion values. The *lme* function within the *nlme* package was used to create and validate the model (Pinheiro *et al.*, 2021), and if fixed effects were found to be significant, post hoc tests (Tukey's HSD) were run using the *glht* function in the *multcomp* package (Hothorn, Bretz, and Westfall, 2008). An alpha (α) value of 0.05 was used unless otherwise noted. Final model structures are described below in the corresponding results sections, and final model values, including predictor coefficients and statistical outputs, are presented in Appendix Tables 1 and 2.

RESULTS

Dissolved nutrient efflux measurements from bioreactor incubations were used to determine the magnitude of the potential of sandy marine sediments to supply recycled nutrients to the overlying water column. These estimates were further informed by *in situ* measurements of porewater and seawater nutrient concentrations. All resulting datasets from these sampling efforts are published and publicly available via the Santa Barbara Coastal Long Term Ecological Research Data Catalog (https://sbclter.msi.ucsb.edu/data/catalog/).

Porewater Nutrient Concentrations and Temperature

Porewater ammonium (NH_4^+) concentrations measured in sediments near kelp forests in June and August 2016 ranged from 12.9 to 66.7μM, and the mean porewater NH_4^+ concentration across all sites and sediment depths sampled was 42.3 ± 15.7 μM (Table 1). NH_4^+ concentrations in sediment porewaters did not increase with sediment depth, except at Arroyo Burro Reef at 15 m water depth and Mohawk Reef at 20 m water depth.

Between 10 August and 1 September 2016, temperatures measured in the sediment ranged from 13.6 to 19.7 °C, and both extrema were measured by the thermistor buried at 5 cm. Water temperatures measured 50 cm above the sediment ranged from 13.3 to 20.0 °C (Figure 2A). The cross-covariance between each sediment temperature logger ($n = 3$) and the overlying water column were computed for the 22-day dataset and the values at which the cross-covariance values were greatest indicate the timestep, or lag, at which there is the strongest correlation between the two time-series (*sensu* Fram *et al.*, 2014). Temperatures at 5 cm depth in the sediment had the strongest correlation with overlying water temperature changes (*i.e.* the highest cross-covariance value) at a 10-minute lag (Figure 2B). At 15 cm sediment depth, the lag was 100 minutes or approximately two hours (Figure 2C). At 30 cm sediment depth, the lag was 1,845 minutes or approximately 31 hours (Figure 2D). These lag times suggest that porewater in the top 5 cm of sediment flushes approximately 144 times daily, porewater at 15 cm depth flushes approximately 14 times daily, and porewater at 30 cm depth flushes approximately once a day.

Seawater NH_4^+ concentrations measured in June and August 2016 ranged from the limit of detection (0.05 μM) to 1.0 μM, and the mean water column NH_4^+ concentration at all sites and water depths sampled was 0.3 ± 0.3 μM (Table 2). NH_4^+ concentrations in water sampled near the bottom were greatest in all but one location (Mohawk, 5 m).

Sediment Characteristics

Using the sediment collected between 2017 and 2019 for bioreactor experiments, the mean percent water content of the sediment sampled from the Arroyo Burro, Goleta Bay, and Mission Creek reefs is 34% ± 4.7%, 29% ± 2.5%, and 28.5% ± 1.9%, respectively. Remaining sediment characteristics for the marine sites surveyed between 2015 and 2017 are listed in Table 3 (Santa Barbara Coastal LTER *et al.*, 2018a). The mean percent organic matter at these sites is 1.52% ± 0.47%, with mean percent organic carbon content of 0.47% ± 0.20%. The mean C:N values of these sediments is 10.0 ± 2.4. The median grain size of these sediments is 92.9 μm, and the mean clay, silt, and sand content of these sediments are 5.7% ± 4.1%, 29.3% ± 14.1%, and 65% ± 18, respectively.

Table 2. *Seawater ammonium concentrations (μM) measured near kelp forest sites in summer 2016 (Santa Barbara Coastal LTER et al., 2018b). Exact water sampling depth reported in parentheses, and deeper water depths are located further offshore.*

Water Depth (m)	ABUR 15 m	MICR 15 m	REFU 15 m	MOHK 5 m	7 m	10 m	15 m	20 m
Surface	0.1 (1)	0.1 (1)	0.1 (1)	0.3 (1)	0.2 (1)	0.1 (1)	0.1 (1)	0.1 (1)
Midway	0.1 (7.5)	0.1 (7.5)	0.1 (7.5)	0.4 (2.5)	0.3 (3.5)	0.6 (5.5)	0.1 (6.5)	0.2 (7.5)
Bottom	0.3 (14.5)	1.0 (14.5)	0.2 (14.5)	0.4 (4.5)	0.6 (6.5)	0.7 (10.5)	0.9 (12.5)	0.7 (14.5)

Arroyo Burro = ABUR, Mission Creek = MICR, Refugio = REFU, Mohawk = MOHK

Dissolved Nitrogen Fluxes from Bioreactor Incubations

Ammonium (NH_4^+) concentrations in the seawater used for the bioreactor experiments ranged from 0.1 to 0.9 μM. After performing the experimental runs, NH_4^+ concentrations measured in replicates containing sediment cores ranged from 0.1 to 2.5 μM. A linear mixed effects model with treatment (*i.e.* presence of sediment) as a fixed effect, site as a random effect, and an additional term allowing different variances by treatment indicated that treatment had a significant effect on measured NH_4^+ concentrations ($p = 0.0004$, Appendix Table 1). Furthermore, NH_4^+ fluxes from bioreactors containing sediment were significantly different from those containing only seawater (Tukey's post hoc, $p = 0.0002$, Appendix Table 1). Across all years and sites sampled, the mean net flux of NH_4^+ from kelp forest sediment was 21.6 μmol m^{-2} hr^{-1} (0.52 mmol m^{-2} day^{-1}) from the 0–2 cm sediment horizon, and fluxes from cores at individual sites across all years ranged from 2.2 to 37.3 μmol m^{-2} hr^{-1} (0.05 to 0.90 mmol m^{-2} day^{-1}) (Table 4). All samples measured for NH_4^+ fell above the limit of detection (0.05 μM).

Measurements of nitrate concentrations included both nitrate (NO_3^-) and nitrite (NO_2^-) and are referred to jointly as nitrate or NO_3^-; this is how concentrations are reported by the SBC LTER as part of the monthly sampling campaigns (Santa Barbara Coastal LTER *et al.*, 2021b). NO_3^- concentrations in the kelp forest seawater used for the bioreactor experiments ranged from 0.2 to 1.3 μM. After performing the experimental runs, NO_3^- concentrations measured in replicates containing sediment cores ranged from 0.2 to 1.7 μM. A linear mixed effects model with treatment as a fixed effect and site as a random effect indicated that treatment did not have a significant effect on measured NO_3^- concentration ($p = 0.31$, Appendix Table 1). Despite NO_3^- fluxes from bioreactors with sediment not being significantly different from those containing only seawater, the mean net NO_3^- flux for kelp forest sediments across all sites and years sampled was 8.5 μmol m^{-2} hr^{-1} (0.2 mmol m^{-2} day^{-1}) from the 0-2 cm sediment horizon, and fluxes at individual sites across all years ranged from -18.6 to 27.8 μmol m^{-2} hr^{-1} (−0.45 to 0.67 mmol m^{-2} day^{-1}) (Table 4).

Approximately 27% of the samples ($n = 25$) analyzed for NO_3^- were below the limit of detection (0.50 μM in 2017, 0.20 μM in 2018 and 2019).

In 2018 and 2019, total dissolved nitrogen (TDN) concentrations in the seawater used for the bioreactor experiments ranged from 5.1 to 6.6 μM. After performing the experimental runs, TDN concentrations measured in replicates containing sediment cores ranged from 6.4 to 10.8 μM. A linear mixed effects model with treatment as a fixed effect, site as a random effect, and an additional term allowing different variances by treatment indicated that treatment had a significant effect on measured TDN concentrations ($p < 0.0001$, Appendix Table 1). Furthermore, TDN fluxes from bioreactors containing sediment were significantly different than from those containing only seawater (Tukey's post hoc, $p < 0.0001$, Appendix Table 1). Including both years and all sites sampled, the mean net TDN flux from kelp forest sediment was 79.1 μmol m^{-2} hr^{-1} (1.9 mmol m^{-2} day^{-1}) from the 0–2 cm sediment horizon, and fluxes for individual site-years ranged from 24.8 to 97.5 μmol m^{-2} hr^{-1} (0.6 to 2.3 mmol m^{-2} day^{-1}) (Table 4). All samples measured for TDN were above the limit of detection (2 μM).

Subtracting NH_4^+ and NO_3^- from TDN measurements to estimate DON fluxes, DON fluxes from kelp forest sediment cores were calculated to be approximately 49 μmol m^{-2} hr^{-1} (1.2 mmol m^{-2} day^{-1}) from the 0-2 cm sediment horizon (Table 4).

Diel Water Sampling

In 2018, diel water sampling was scheduled to coincide with neap, midway, and spring tide conditions on August 3, 7, and 10, respectively, to account for the full range of tidal heights in relationship to NH_4^+ concentrations (Santa Barbara Coastal LTER *et al.*, 2021a). Published tidal heights ranged from –0.31 m to 2.23 m; both extrema occurred during the last sampling campaign on August 10 to 11 (NOAA, 2020) (Figure 3). The mean water temperature during diel sampling was 19.78 °C and ranged from 16.86 °C to 22.84 °C (Figure 3).

The mean NH_4^+ concentration of all depths and times was 0.7 ± 0.5 μM, and concentrations ranged from the limit of detection (0.05 μM) to 2.0 μM (Figure 3). Concentrations were typically highest in the early morning (0200–0600), decreased through-

Table 3. *Marine sediment characteristics based on sediment cores collected from 2015 to 2017 in the nearshore Santa Barbara Channel (20 m water depth) (Santa Barbara Coastal LTER et al., 2018a). Characteristics include organic matter (OM) content and stoichiometric content (Carbon:Nitrogen).*

Site	% OM	C:N	% Clay	% Silt	% Sand	Median Grain Size (μm)
ABUR	1.9 ± 0.5	11.8 ± 2.8	4.3 ± 0.6	30.9 ± 4.1	64.7 ± 4.6	77.8 ± 4.8
GOLB	1.1 ± 0.2	8.3 ± 1.3	3.2 ± 0.3	17.3 ± 2.4	79.5 ± 2.7	121.4 ± 7.3
MICR	1.5 ± 0.3	8.9 ± 1.1	10.0 ± 3.9	40.2 ± 15.2	49.8 ± 19.1	89.5 ± 63.3
MOHK	1.5 ± 0.3	11.0 ± 2.5	5.9 ± 5.4	29.7 ± 18.5	64.5 ± 23.7	89.2 ± 31.1
REFU	1.6 ± 0.5	10.2 ± 2.3	5.2 ± 3.9	28.2 ± 12.4	66.6 ± 16.2	86.6 ± 21.6

Arroyo Burro = ABUR, Mission Creek = MICR, Refugio = REFU, Mohawk = MOHK

Table 4. *Mean dissolved nutrient fluxes (μmol m^{-2} hr^{-1}) measured using sediment cores from kelp forest sites in August 2017, 2018, and 2019.*

		Measured			Calculated
Year	Site	NH$_4^+$	NO$_3^-$	TDN	DON
2017	ABUR	25.7	−10.0	—	—
2017	GOLB	37.3	11.9	—	—
2017	MICR	36.5	4.7	—	—
2018	ABUR	12.8	9.4	92.6	70.4
2018	GOLB	2.2	8.1	73.0	62.7
2018	MICR	7.3	27.8	93.5	58.4
2019	ABUR	12.8	−18.6	24.8	30.5
2019	GOLB	31.3	22.0	97.5	44.2
2019	MICR	28.8	21.1	93.3	43.4

Arroyo Burro = ABUR, Mission Creek = MICR, Refugio = REFU, Mohawk = MOHK

out the day (1000–1800), and increased during the night (2200–0200). The mean NO$_3^-$ concentration measured was 0.2 ± 0.04 μM, and concentrations ranged from 0.2 μM to 0.4 μM (Figure 3). NO$_3^-$ concentrations remained low (<0.4 μM) and were nearly always an order of magnitude less than NH$_4^+$ concentrations. The mean chlorophyll *a* concentration was 1.5 ± 0.7 μg L^{-1}, and concentrations ranged from 0.6 to 4.1 μg L^{-1} (Figure 3).

A linear mixed effects model created to predict NH$_4^+$ concentrations included tidal height and temperature as interacting fixed effects, chlorophyll *a* as another fixed effect, and water depth as a random effect. The interaction term between tides and temperature was not significant ($p = 0.08$), but there was a significant effect of tidal height, temperature, and chlorophyll *a* on NH$_4^+$ concentrations ($p < 0.001$ for all). Model coefficients further suggest NH$_4^+$ concentrations were inversely related to tidal height, temperature, and chlorophyll *a* (Appendix Table 2).

DISCUSSION

Measurements of porewater, seawater, and marine sediment effluxes indicate that when other mechanisms of nutrient delivery, such as upwelling, are infrequent or not occurring, nutrient regeneration by permeable marine sediments can play a role in meeting nutrient demand in SBC kelp forest ecosystems. *In situ* porewater and water column measurements suggest sediment porewaters and overlying water contain appreciable concentrations of ammonium (NH$_4^+$)
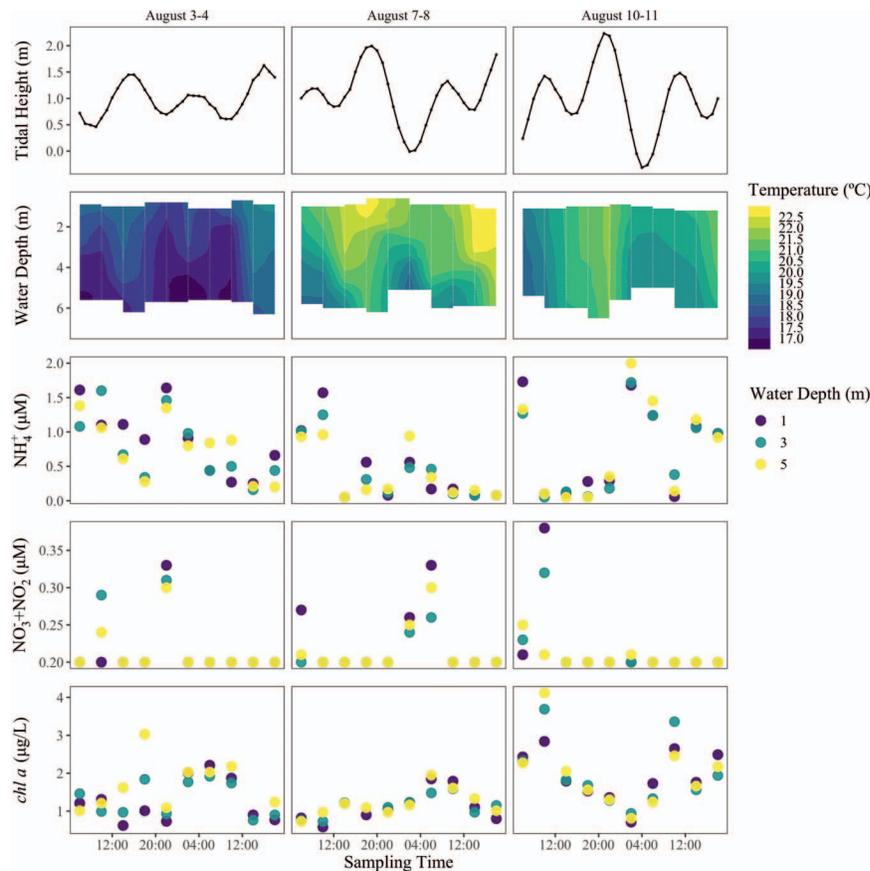
Figure 3. Tidal height, temperature, ammonium (NH$_4^+$) concentrations, nitrate/nitrite (NO$_3^-$/NO$_2^-$) concentrations, and chlorophyll a concentrations of seawater for sampling dates in August 2018 (Santa Barbara Coastal LTER *et al.*, 2021a). Neap midway, and spring tide conditions occurred during the August 3–4, 7–8, and 10–11 sampling dates, respectively. Vertical dashed white lines on temperature panels indicate sampling times.
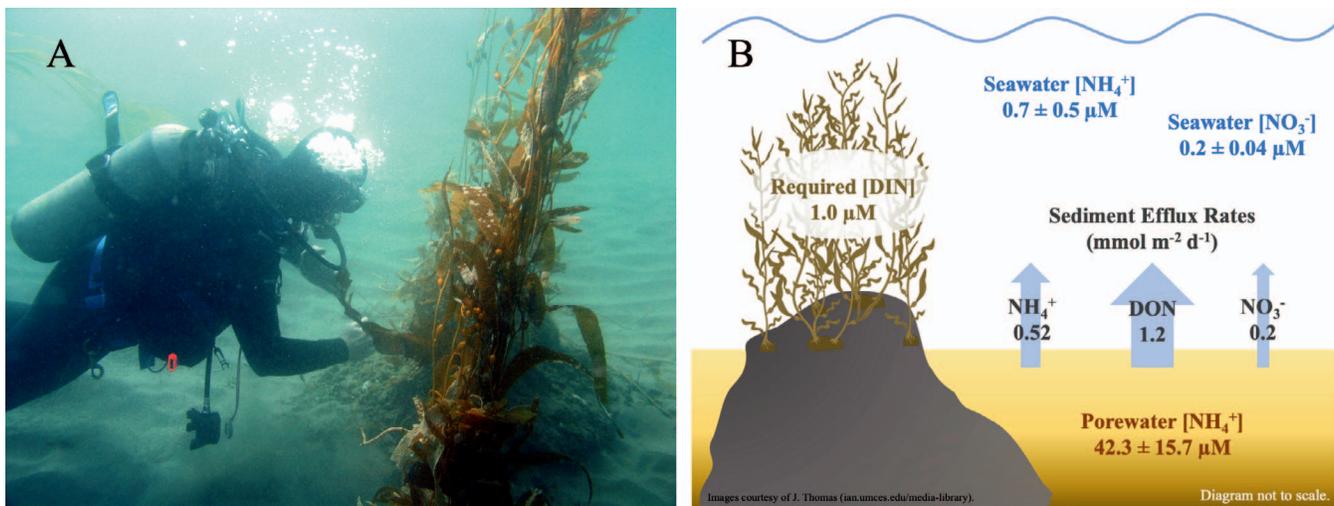
Figure 4. Panel A depicts a diver sampling near giant kelp surrounded by sandy sediment in the Santa Barbara Channel (photo courtesy of Clint Nelson, Santa Barbara Coastal Long Term Ecological Research). Panel B depicts a conceptual figure of dissolved nitrogen pools and fluxes in the nearshore of the Santa Barbara Channel during the summer season. Minimum required dissolved inorganic nitrogen (DIN) concentration as reported by Gerard *et al.* (1982b). Ammonium (NH_4^+) concentrations (mean $\pm$ s.d.) were measured in sediment porewater in July and August 2016. NH_4^+ and nitrate/nitrite (NO_3^-/NO_2^-) concentrations (mean $\pm$ s.d.) were measured in overlying seawater in August 2018. Fluxes of dissolved nitrogen species (mean) from sediment surrounding kelp forests were measured using sediment core incubations in August 2017–2019.

(Santa Barbara Coastal LTER *et al.*, 2018b), and porewater temperatures demonstrated rapid exchange across the sediment-water interface (Santa Barbara Coastal LTER *et al.*, 2018c). Fluxes from bioreactors are similar to sediment effluxes in comparable nearshore marine environments and indicate that permeable marine sediments around giant kelp forests in the SBC can serve as a net source of nutrients to the overlying water (Figure 4).

In situ measurements of porewater chemistry and temperature in nearshore SBC marine sediments indicate that these sediments are replete with dissolved inorganic nitrogen and flush regularly. SBC sediments have ammonium (NH_4^+) concentrations that are several orders of magnitude greater than in the overlying water (Tables 1 and 2). Previous studies examining SBC beach porewater nutrient concentrations also found NH_4^+ to be the dominant form of dissolved inorganic nitrogen, with concentrations several orders of magnitude greater than nearshore seawater (Goodridge and Melack, 2014; Lowman *et al.*, 2019). In addition, SBC sediment porewaters at 5 cm, 15 cm, and 30 cm depths flush roughly at minute, hourly, and daily rates, decreasing exponentially with increasing sediment depth (Figure 2). In another study of permeable sediment porewater flushing done in a Mediterranean lagoon, water was found to exchange to a depth of 25 cm on an approximately daily basis, and porewater exchange was found to decay exponentially with depth (Cook *et al.*, 2018). Frequent flushing of porewater maintains aerobic conditions suitable for microbial ammonification and nitrification (Capone *et al.*, 2008; Woulds *et al.*, 2016), prevents significant rates of anaerobic processing such as annamox (Herbert, 1999), and stimulates remineralization as the redox boundary oscillates (Rocha, 2008). In this study, NH_4^+ concentrations were examined as a proxy for organic matter remineralization (Laverman *et al.*,

2012), and data suggest that with regular flushing, these permeable marine sediments have the capacity to rapidly regenerate dissolved nutrient concentrations. Due to the high porewater nutrient concentrations (>40 μM NH_4^+) and rapid turnover of sediment porewater (minutes to days), sediments in the SBC are well-suited to routinely resupply the overlying water with dissolved nitrogen that can be taken up to support primary productivity in giant kelp forests.

The bioreactor results demonstrated the sediments' ability to serve as a source of dissolved nitrogen. Across all sites and years, mean fluxes measured in the bioreactors were 0.52 mmol NH_4^+ m^{-2} day^{-1} (0.05 to 0.90 mmol m^{-2} day^{-1}), 0.20 mmol NO_3^- m^{-2} day^{-1} (−0.45 to 0.67 mmol m^{-2} day^{-1}), and 1.90 mmol TDN m^{-2} day^{-1} (0.60 to 2.34 mmol m^{-2} day^{-1}) (Table 3). These fluxes are comparable to other published values using incubations of coastal marine sediment cores (Boynton *et al.*, 2018; Capone *et al.*, 2008). In particular, NH_4^+ effluxes from kelp forest sediments were of a similar magnitude as values measured in the nearshore Georgia Bight (1.38 mmol m^{-2} day^{-1}), although rates in this region are likely higher since water temperatures may reach 28 °C (Hopkinson, 1987). The NH_4^+ effluxes measured in our bioreactors suggest that, in a 10 m deep water column with an average NH_4^+ concentration of 0.7 μM (Figure 3), the 0–2 cm horizon is capable of supplying 1–13% of the NH_4^+ available in the overlying water column. The results of the bioreactor incubations demonstrate that across multiple years and sites, nearshore permeable marine sediments in the SBC are a net source of dissolved nitrogen, most notably NH_4^+, to the overlying water during the summer season.

Other studies using *in situ* chambers, batch incubations, and flow-through cores in estuarine and marine sediment report higher NH_4^+ effluxes (Boynton *et al.*, 2018), and the NH_4^+ effluxes measured in this study would likely also be greater if

the sediment depths considered were extended from the 0–2 cm horizon used in the bioreactor setup to the 0–30 cm horizon demonstrated to flush regularly in this system. However, since flushing and remineralization rates likely both vary with depth, while our incubations were done in the top 2 cm, and due to heterogeneity in microbial and macrofaunal communities, fluxes were not extrapolated to depth. Using the effluxes measured from the top 2 cm of sediment, the NH_4^+ fluxes are comparable to reported excretion rates by sessile and mobile benthic invertebrates, which may contribute 3.5 to 18.3 μmol NH_4^+ m^{-2} hr^{-1} via excretion in nearshore SBC kelp forests (Peters, Reed, and Burkepile, 2019). These values, and the calculated sediment effluxes ranging from 2.2 to 37.3 NH_4^+ μmol m^{-2} hr^{-1} (0.05 to 0.90 mmol m^{-2} day^{-1}) indicate that invertebrate excretion and microbial remineralization in permeable sediments are both important sources of dissolved nitrogen that may support giant kelp growth in low-nutrient conditions.

To further examine nitrogen availability during low-nutrient, stratified periods, diel sampling was conducted in the nearshore region of the SBC. Measurements from August 2018 confirm a consistent presence of NH_4^+, with concentrations exceeding 1 μM during 33% of the diel sampling events ($n = 10$, Figure 3) (Santa Barbara Coastal LTER *et al.*, 2021a). This concentration is above a threshold of 1 μM dissolved inorganic nitrogen below which giant kelp growth cannot support the average growth rate of 4% day^{-1} (Gerard, 1982b). In addition to measuring NH_4^+ concentrations above 1 μM for several hours during each sampling campaign, a diel pattern occurred, with lower ambient NH_4^+ concentrations during the day and higher concentrations at night (Santa Barbara Coastal LTER *et al.*, 2021a). Previous sampling in kelp forests of the SBC also demonstrate a distinct diel periodicity in NH_4^+ concentrations throughout the entire water column (Brzezinski *et al.*, 2013). This same pattern has been reported in nearby surface waters of the Southern California Bight, where NH_4^+ regeneration rates were found to be highest at night (Bronk and Ward, 2005; Ward and Bronk, 2001). Together, these diel sampling data suggest a greater presence of recycled nitrogen (*i.e.* NH_4^+) during stratified conditions in the SBC than previously recognized.

CONCLUSIONS

Based on *in situ* sampling and sediment bioreactor incubations, data suggest NH_4^+ effluxes from permeable sediments around giant kelp forests are an important source of nutrients for primary producers in the coastal SBC. All sampling took place during the stratified summer season, when water temperatures in the SBC are greatest and NO_3^- concentrations are lowest (Brzezinski *et al.*, 2013; McPhee-Shaw *et al.*, 2007). Fluxes of chemical species from sediment change seasonally (Nielsen, Risgaard-Petersen, and Banta, 2017; Smyth *et al.*, 2018), and nutrient fluxes from marine sediment have been demonstrated to increase with increasing temperatures in summer (Boynton *et al.*, 2018) as well as with increased mixing and resuspension in winter (Wei *et al.*, 2022). Sediments in the SBC may have the capacity for increased remineralization rates during winter, when wave energy is higher and more organic material is delivered to the coast due to storms, but

these are also periods of high NO_3^- availability when contributions of NH_4^+ are less important (Aguilera and Melack, 2018; Brzezinski *et al.*, 2013). In summer, during higher water temperatures and lower nutrient concentrations, sediments possess the potential to serve as a key source of recycled nutrients to giant kelp forests and other primary producers. Furthermore, the results of this study are among the first to demonstrate that giant kelp forests may be exposed to NH_4^+ concentrations >1 μM for multiple hours over the course of a day during summer months. This finding is of particular note since it has been demonstrated that giant kelp rapidly uptakes NH_4^+ during pulse exposure in the summer months (Cedeno *et al.*, 2021). Globally, giant kelp forests are recognized as productive, diverse ecosystems, but some are declining due to rising seawater temperatures (Johnson *et al.*, 2011; Raybaud *et al.*, 2013), which has also been linked to declining nutritional content (C:N) of giant kelp (Lowman *et al.*, 2021a). Studies such as this one regarding nutrient availability to support giant kelp growth are critical for forecasting the resilience of giant kelp in the face of increasing abiotic stress, specifically periods of higher seawater temperatures and lower dissolved nutrient concentrations.

LITERATURE CITED

Aguilera, R. and Melack, J.M., 2018. Relationships among nutrient and sediment fluxes, hydrological variability, fire, and land cover in coastal California catchments. *Journal of Geophysical Research: Biogeosciences*, 123(8), 2568–2589.

Ahmerkamp, S.; Winter, C.; Krämer, K.; de Beer, D.; Janssen, F.; Friedrich, J.; Kuypers, M.M.M., and Holtappels, M., 2017. Regulation of benthic oxygen fluxes in permeable sediments of the coastal ocean. *Limnology and Oceanography*, 62(5), 1935–1954.

Boudreau, B.P.; Huettel, M.; Forster, S.; Jahnke, R.A.; McLachlan, A.; Middelburg, J.J.; Nielsen, P.; Sansone, F.; Taghon, G.; Van Raaphorst, W.; Webster, I.; Weslawski, J.M.; Wiberg, P., and Sundby, B., 2001. Permeable marine sediments: Overturning an old paradigm. *EOS Transactions American Geophysical Union,* 82(11), 133–140.

Boynton, W.R.; Ceballos, M.A.C.; Bailey, E.M.; Hodgkins, C.L.S.; Humphrey, J.L., and Testa, J.M., 2018. Oxygen and nutrient exchanges at the sediment-water interface: A global synthesis and

critique of estuarine and coastal data. *Estuaries and Coasts*, 41(2), 301–333.

Bronk, D.A. and Ward, B.B., 2005. Inorganic and organic nitrogen cycling in the Southern California Bight. *Deep Sea Research Part I: Oceanographic Research Papers*, 52(12), 2285–2300.

Brzezinski, M.; Reed, D.; Harrer, S.; Rassweiler, A.; Melack, J.; Goodridge, B., and Dugan, J., 2013. Multiple sources and forms of nitrogen sustain year-round kelp growth on the inner continental shelf of the Santa Barbara Channel. *Oceanography,* 26(3), 114–123.

Cai, P.; Wei, L.; Geibert, W.; Koehler, D.; Ye, Y.; Liu, W., and Shi, X., 2020. Carbon and nutrient export from intertidal sand systems elucidated by 224Ra/228Th disequilibria. *Geochimica et Cosmochimica Acta*, 274, 302–316.

Capone, D.G.; Bronk, D.A.; Mulholland, M.R., and Carpenter, E.J., 2008. *Nitrogen in the Marine Environment*, 2nd edition. New York: Academic Press, 1729p.

Cedeno, T.H.; Brzezinski, M.A.; Miller, R.J., and Reed, D.C. 2021. An evaluation of surge uptake capability in the giant kelp (*Macrocystis pyrifera*) in response to pulses of three different forms of nitrogen. *Marine Biology*, 168, 166.

Cook, P.G.; Rodellas, V.; Andrisoa, A., and Stieglitz, T.C., 2018. Exchange across the sediment-water interface quantified from porewater radon profiles. *Journal of Hydrology*, 559, 873–883.

Cook, P.L.M.; Wenzhöfer, F.; Rysgaard, S.; Galaktionov, O.S.; Meysman, F.J.R.; Eyre, B.D.; Cornwell, J.; Huettel, M., and Glud, R.N., 2006. Quantification of denitrification in permeable sediments: Insights from a two-dimensional simulation analysis and experimental data: Denitrification in permeable sediments. *Limnology and Oceanography Methods*, 4, 294–307.

de Beer, D.; Wenzhöfer, F.; Ferdelman, T.G.; Boehme, S.E.; Huettel, M.; van Beusekom, J.E.; Böttcher, M.E.; Musat, N., and Dubilier, N., 2005. Transport and mineralization rates in North Sea sandy intertidal sediments, Sylt-Rm Basin, Wadden Sea. *Limnology and Oceanography*, 50, 113–127.

Dunnington, D., 2020. *ggspatial: Spatial data framework for ggplot2. R package version 1.1.5*. https://CRAN.R-project.org/package=ggspatial

Falter, J.L. and Sansone, F.J., 2000. Hydraulic control of pore water geochemistry within the oxic-suboxic zone of a permeable sediment. *Limnology and Oceanography*, 45(3), 550–557.

Fewings, M.R.; Washburn, L., and Ohlmann, J.C., 2015. Coastal water circulation patterns around the Northern Channel Islands and Point Conception, California. *Progress in Oceanography*, 138, 283–304.

Fram, J.P.; Pawlak, G.R.; Sansone, F.J.; Glazer, B.T., and Hannides, A.K., 2014. Miniature thermistor chain for determining surficial sediment porewater advection. *Limnology and Oceanography: Methods*, 12, 155–165.

Fram, J.P.; Stewart, H.L.; Brzezinski, M.A.; Gaylord, B.; Reed, D.C.; Williams, S.L., and MacIntyre, S., 2008. Physical pathways and utilization of nitrate supply to the giant kelp, *Macrocystis pyrifera*. *Limnology and Oceanography*, 53(4), 1589–1603.

Gerard, V.A., 1982a. Growth and utilization of internal nitrogen reserves by the giant kelp *Macrocystis pyrifera* in a low-nitrogen environment. *Marine Biology*, 66(1), 27–35.

Gerard, V.A., 1982b. In situ rates of nitrate uptake by giant kelp, *Macrocystis pyrifera* (L.) C. Agardh: Tissue differences, environmental effects, and predictions of nitrogen-limited growth. *Journal of Experimental Marine Biology and Ecology*, 62, 211–224.

Glibert, P.M.; Wilkerson, F.P.; Dugdale, R.C.; Raven, J.A.; Dupont, C.L.; Leavitt, P.R.; Parker, A.E.; Burkholder, J.M., and Kana, T.M., 2016. Pluses and minuses of ammonium and nitrate uptake and assimilation by phytoplankton and implications for productivity and community composition, with emphasis on nitrogen-enriched conditions. *Limnology and Oceanography,* 61(1), 165–197.

Goodridge, B.M. and Melack, J.M., 2014. Temporal evolution and variability of dissolved inorganic nitrogen in beach pore water revealed using radon residence times. *Environmental Science and Technology,* 48(24), 14211–14218.

Gustafsson, C. and Norkko, A., 2016. Not all plants are the same: Exploring metabolism and nitrogen fluxes in a benthic community composed of different aquatic plant species. *Limnology and Oceanography,* 61(5), 1787–1799.

Herbert, R.A., 1999. Nitrogen cycling in coastal marine ecosystems. *FEMS Microbiology Reviews*, 23, 563–590.

Holmes, R.M.; Aminot, A.; Kérouel, R.; Hooker, B.A., and Peterson, B.J., 1999. A simple and precise method for measuring ammonium in marine and freshwater ecosystems. *Canadian Journal of Fisheries and Aquatic Sciences*, 56(10), 1801–1808.

Hopkinson, J., 1987. Nutrient regeneration in shallow-water sediments of the estuarine plume region of the nearshore Georgia Bight. *Marine Biology*, 94, 127–142.

Hothorn, T.; Bretz, F., and Westfall, P., 2008. Simultaneous inference in general parametric models. *Biometrical Journal*, 50(3), 346–363.

Huettel, M.; Berg, P., and Kostka, J.E., 2014. Benthic exchange and biogeochemical cycling in permeable sediments. *Annual Review of Marine Science*, 6(1), 23–51.

Janssen, F.; Huettel, M., and Witte, U., 2005. Pore-water advection and solute fluxes in permeable marine sediments (II): Benthic respiration at three sandy sites with different permeabilities (German Bight, North Sea). *Limnology and Oceanography*, 50(3), 779–792.

Johnson, C.R.; Banks, S.C.; Barrett, N.S.; Cazassus, F.; Dunstan, P.K.; Edgar, G.J.; Frusher, S.D.; Gardner, C.; Haddon, M.; Helidoniotis, F.; Hill, K.L.; Holbrook, N.J.; Hosie, G.W.; Last, P.R.; Ling, S.D.; Melbourne-Thomas, J.; Miller, K.; Pecl, G.T.; Richardson, A.J.; Ridgway, K.R.; Rintoul, S.R.; Ritz, D.A.; Ross, D.J.; Sanderson, J.C.; Shepherd, S.A.; Slotwinski, A.; Swadling, K.M., and Taw, N., 2011. Climate change cascades: Shifts in oceanography, species' ranges and subtidal marine community dynamics in eastern Tasmania. *Journal of Experimental Marine Biology and Ecology*, 400, 17–32.

Kahle, D. and Wickham, H., 2013. gmap: Spatial visualization with ggplot2. *The R Journal*, 5(1), 144–161. http://journal.r-project.org/archive/2013-1/kahle-wickham.pdf

Kessler, A.J.; Glud, R.N.; Cardenas, M.B.; Larsen, M.; Bourke, M.F., and Cook, P.L.M., 2012. Quantifying denitrification in rippled permeable sands through combined flume experiments and modeling. *Limnology and Oceanography*, 57, 1217–1232.

Kitidis, V.; Tait, K.; Nunes, J.; Brown, I.; Woodward, E.M.S.; Harris, C.; Sabadel, A.J.M.; Sivyer, D.B.; Silburn, B., and Kröger, S., 2017. Seasonal benthic nitrogen cycling in a temperate shelf sea: the Celtic Sea. *Biogeochemistry*, 135, 103–119.

Laverman, A.M.; Pallud, C.; Abell, J., and Cappellen, P.V., 2012. Comparative survey of potential nitrate and sulfate reduction rates in aquatic sediments. *Geochimica et Cosmochimica Acta*, 77, 474–488.

Lowman, H.; Moingt, M.; Lucotte, M.; Melack, J., and Page, H.M., 2021b. Terrestrial organic matter inputs to nearshore marine sediment under prolonged drought followed by significant rainfall as indicated by lignin. *Estuaries and Coasts*, 44, 2159–2172.

Lowman, H.E.; Emery, K.A.; Dugan, J.E., and Miller, R.J., 2021a. Nutritional quality of giant kelp declines due to warming ocean temperatures. *Oikos*. https://doi.org/10.1111/oik.08619

Lowman, H.E.; Emery, K.A.; Kubler-Dudgeon, L.; Dugan, J.E., and Melack, J.M., 2019. Contribution of macroalgal wrack consumers to dissolved inorganic nitrogen concentrations in intertidal pore waters of sandy beaches. *Estuarine, Coastal and Shelf Science*, 219, 363–371.

Marchant, H.K.; Holtappels, M.; Lavik, G.; Ahmerkamp, S.; Winter, C., and Kuypers, M.M.M., 2016. Coupled nitrification-denitrification leads to extensive N loss in subtidal permeable sediments. *Limnology and Oceanography*, 61(3), 1033–1048.

McPhee-Shaw, E.E.; Siegel, D.A.; Washburn, L.; Brzezinski, M.A.; Jones, J.L.; Leydecker, A., and Melack, J., 2007. Mechanisms for nutrient delivery to the inner shelf: Observations from the Santa Barbara Channel. *Limnology and Oceanography*, 52(5), 1748–1766.

Mullen, L.A. and Bratt, J., 2018. USA boundaries: Historical and contemporary boundaries of the United States of America. *Journal of Open Source Software*, 3(23), 314.

National Oceanographic and Atmospheric Administration (NOAA), 2020. *Tides & Currents: Station ID 9411340*. https://tidesandcurrents.noaa.gov/waterlevels.html?id=9411340

Nielsen, S.L.; Risgaard-Petersen, N., and Banta, G.T., 2017. Nitrogen retention in coastal marine sediments—A field study of the relative importance of biological and physical removal in a Danish estuary. *Estuaries and Coasts,* 40(5), 1276–1287.

Page, H.; Reed, D.; Brzezinski, M.; Melack, J., and Dugan, J., 2008. Assessing the importance of land and marine sources of organic matter to kelp forest food webs. *Marine Ecology Progress Series*, 360, 47–62.

Pallud, C.; Meile, C.; Laverman, A.M.; Abell, J., and Van Cappellen, P., 2007. The use of flow-through sediment reactors in biogeochemical kinetics: Methodology and examples of applications. *Marine Chemistry*, 106, 256–271.

Pallud, C. and Van Cappellen, P., 2006. Kinetics of microbial sulfate reduction in estuarine sediments. *Geochimica et Cosmochimica Acta*, 70, 1148–1162.

Pebesma, E., 2018. Simple features for R: Standardized support for spatial vector data. *The R Journal*, 10(1), 439–446.

Peters, J.R.; Reed, D.C., and Burkepile, D.E., 2019. Climate and fishing drive regime shifts in consumer-mediated nutrient cycling in kelp forests. *Global Change Biology*, 25(9), 3179–3192.

Pinheiro, J.; Bates, D.; DebRoy, S.; Sarkar, D., and R Core Team, 2021. *nlme: Linear and nonlinear mixed effects models. R package version 3.1-153*. https://CRAN.R-project.org/package=nlme

Poppe, L.J.; Eliason, A.H.; Frederick, J.J.; Rendigs, R.R.; Blackwood, D., and Polloni, C.F., 2000. USGS East-Coast sediment analysis: Procedures, database, and georeferenced displays (Open-File No. 00-358). U.S. Geological Survey. https://doi.org/10.3133/ofr00358

R Core Team, 2021. *R: A language and environment for statistical computing*. R Foundation for Statistical Computing, Vienna, Austria. https://www.R-project.org/

Raybaud, V.; Beaugrand, G.; Goberville, E.; Delebecq, G.; Destombe, C.; Valero, M.; Davoult, D.; Morin, P., and Gevaert, F., 2013. Decline in kelp in West Europe and climate. *PLoS ONE,* 8(6), 1–10.

Reed, D.; Washburn, L.; Rassweiler, A.; Miller, R.; Bell, T., and Harrer, S., 2016. Extreme warming challenges sentinel status of kelp forests as indicators of climate change. *Nature Communications*, 7, 13757.

Rocha, C., 2008. Sandy sediments as active biogeochemical reactors: compound cycling in the fast lane. *Aquatic Microbial Ecology*, 53, 119–127.

Rowe, G.T.; Clifford, C.H., and Smith, K.L., 1975. Benthic nutrient regeneration and its coupling to primary productivity in coastal waters. *Nature*, 255, 215–217.

Roychoudhury, A.N.; Viollier, E., and Van Cappellen, P., 1998. A plug flow-through reactor for studying biogeochemical reactions in undisturbed sediments. *Applied Geochemistry*, 13, 269–280.

Santa Barbara Coastal LTER; Lowman, H.; Melack, J., and Brzezinski, M., 2021a. SBC LTER: Ocean: Diel nearshore water profiles (CTD and chemistry) during stratified conditions ver 1. Environmental Data Initiative. https://doi.org/10.6073/pasta/7a41a41c52b425c564de7aa079839049

Santa Barbara Coastal LTER; Page, H.; Lowman, H.; Melack, J.; Smith, J., and Reed, D., 2018a. SBC LTER: OCEAN: Particulate Organic Matter Content and Composition of Stream, Estuarine, and Marine Sediments ver 1. Environmental Data Initiative. https://doi.org/10.6073/pasta/05ca288d7203107bddab618e95524c0a

Santa Barbara Coastal LTER; Reed, D.C., and Miller, R.J., 2022. SBC LTER: Reef: Kelp forest community dynamics: Abundance and size of giant kelp (Macrocystis Pyrifera), ongoing since 2000 ver 25. *Environmental Data Initiative*. https://doi.org/10.6073/pasta/e6d6196d4f28f5c610ddbce1920780d1

Santa Barbara Coastal LTER; Smith, J.M.; Reed, D.C., and Melack, J.M., 2018b. SBC LTER: OCEAN: Sediment porewater ammonium and urea concentrations ver 4. *Environmental Data Initiative*. https://doi.org/10.6073/pasta/deb7e37cb76c0da76de533dc64c5e383

Santa Barbara Coastal LTER; Smith, J.M.; Reed, D.C., and Melack, J.M., 2018c. SBC LTER: OCEAN: Time series of sediment temperatures by depth ver 3. *Environmental Data Initiative*. https://doi.org/10.6073/pasta/f03abadcd706d64dda456352d311f0c1

Santa Barbara Coastal LTER; Washburn, L.; Brzezinski, M.A.; Carlson, C.A., and Siegel, D.A., 2021b. SBC LTER: Ocean: Ocean Currents and Biogeochemistry: Nearshore water profiles (monthly CTD and chemistry) ver 25. *Environmental Data Initiative*. https://doi.org/10.6073/pasta/d9215920af1305ff9ecfb98fffbe1c2a

Smith, J.M.; Blasco, G.; Brzezinski, M.A.; Melack, J.M.; Reed, D.C., and Miller, R.J., 2020. Factors influencing urea use by giant kelp (*Macrocystis pyrifera*, Phaeophyceae). *Limnology and Oceanography*, 66(4),1190–1200.

Smith, J.M.; Brzezinski, M.A.; Melack, J.M.; Miller, R.J., and Reed, D.C., 2018. Urea as a source of nitrogen to giant kelp (*Macrocystis pyrifera*). *Limnology and Oceanography Letters*, 3(4), 365–373.

Smith, R.C.; Baker, K.S., and Dustan, P., 1981. *Fluorometric Techniques for the Measurement of Oceanic Chlorophyll in the Support of Remote Sensing*. La Jolla, California: Visibility Laboratory, Scripps Institution of Oceanography, University of California, San Diego, pp. 81–117.

Smyth, A.R.; Murphy, A.E.; Anderson, I.C., and Song, B., 2018. Differential effects of bivalves on sediment nitrogen cycling in a shallow coastal bay. *Estuaries and Coasts*, 41(4), 1147–1163.

Sommerfield, C.K.; Lee, H.J., and Normark, W.R., 2009. Postglacial sedimentary record of the Southern California continental shelf and slope, Point Conception to Dana Point. *In*: Lee, H.J. and Normark, W.R. (eds.), *Earth Science in the Urban Ocean: The Southern California Continental Borderland*. Geological Society of America Special Paper 454, pp. 89–115.

Strickland, J.D.H. and Parsons, T.R., 1968. *A Practical Handbook of Seawater Analysis*. Ottawa: Fisheries Research Board of Canada, 310p.

Taylor, B.W.; Keep, C.F.; Hall Jr., R.O.; Koch, B.J.; Tronstad, L.M.; Flecker, A.S., and Ulseth, A.J., 2007. Improving the fluorometric ammonium method: matrix effects, background fluorescence, and standard additions. *Journal of the North American Benthological Society*, 26(2), 167–177.

Ward, B. and Bronk, D., 2001. Net nitrogen uptake and DON release in surface waters: Importance of trophic interactions implied from size fractionation experiments. *Marine Ecology Progress Series*, 219, 11–24.

Wei, L.; Cai, P.; Shi, X.; Cai, W.-J.; Liu, W.; Hong, Q.; Wu, T.; Bai, Y.; Cheng, P., and Sun, Z., 2022. Winter mixing accelerates decomposition of sedimentary organic carbon in seasonally hypoxic coastal seas. *Geochimica et Cosmochimica Acta*, 317, 457–471.

Wheeler, P.A. and North, W.J., 1980. Effect of nitrogen supply on nitrogen content and growth rate of juvenile *Macrocystic Pyrifera* (Phaeophyta) sporophytes. *Journal of Phycology*, 16, 577–582.

Wickham, H.; Averick, M.; Bryan, J.; Chang, W.; D'Agostino McGowan, L.; François, R.; Grolemund, G.; Hayes, A.; Henry, L.; Hester, J.; Kuhn, M.; Pedersen, T.L.; Miller, E.; Bache, S.M.; Müller, K.; Ooms, J.; Robinson, D.; Seidel, D.P.; Spinu, V.; Takahashi, K.; Vaughan, D.; Wilke, C.; Woo, K., and Yutani, H., 2019. Welcome to the Tidyverse. *Journal of Open Source Software,* 4(43), 1686. https://doi.org/10.21105/joss.01686

Woulds, C.; Bouillon, S.; Cowie, G.L.; Drake, E.; Middelburg, J.J., and Witte, U., 2016. Patterns of carbon processing at the seafloor: the role of faunal and microbial communities in moderating carbon flows. *Biogeosciences*, 13(15), 4343–4357.

Zuur, A.F.; Ieno, E.N.; Walker, N.J.; Saveliev, A.A., and Smith, G.M. (eds.), 2009. *Mixed Effects Models and Extensions in Ecology with R*. New York: Springer, 574p.

APPENDIX

Appendix Table 1. *Linear mixed effects model results for standardized nutrient fluxes from sediment bioreactors. Significant fixed effects are denoted in bold.*

Dependent Variable	Fixed Effect	Coefficient	df	F	p
$NH_4^+{}_{standardized}$	Treatment	0.83	1, 53	14.22	**0.0004**
$NO_3^-{}_{standardized}$	Treatment	0.27	1, 53	1.07	0.31
$TDN_{standardized}$	Treatment	1.46	1, 39	44.75	**<0.0001**

Appendix Table 2. *Linear mixed effects model results for log-transformed ammonium (NH_4^+) concentrations (μM) measured during diel sampling. Significant fixed effects are denoted in bold.*

Dependent Variable	Fixed Effect	Coefficient	df	F	p
$\log(NH_4^+)$	Tidal Height * Temperature	0.10	1, 81	3.08	0.0830
	Tidal Height	−2.43	1, 81	38.97	**<0.0001**
	Temperature	−0.24	1, 81	24.24	**<0.0001**
	$\log(chl\ a)$	−0.79	1, 81	15.24	**0.0002**
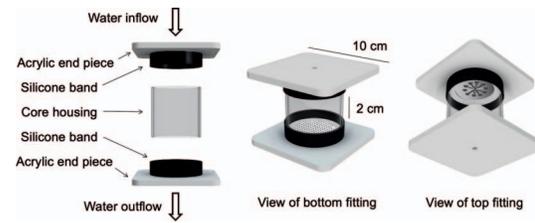
Appendix Figure 1. Flow-through sediment bioreactor design manufactured by laser cutting acrylic sheets for sediment bioreactor incubations performed in 2018 and 2019. This entire setup was connected to a seawater reservoir via PTFE tubing and run using a peristaltic pump. Bioreactor housings used in 2017 followed a similar design but were manufactured by hand. All designs are modified from the flow-through plug design developed by Roychoudhury, Viollier, and Van Cappellen (1998).